ERNEST ORLANDO LAWRENCE
BERKELEY NATIONAL LABORATORY

Critical Temperatures and Pressures for Hydrocarbon Mixtures from an Equation of State with Renormalization-Group-Theory Corrections

J. Jiang and J.M. Prausnitz

Chemical Sciences Division

November 1999

DISCLAIMER

Critical Temperatures and Pressures for Hydrocarbon Mixtures from an Equation of State with Renormalization-Group-Theory Corrections

J. Jiang and J. M. Prausnitz

Department of Chemical Engineering

University of California

and

Chemical Sciences Division

Lawrence Berkeley National Laboratory

University of California

Berkeley, CA 94720, U.S.A.

November 1999

recycled paper

Critical temperatures and pressures for hydrocarbon mixtures from an equation of state with renormalization-group-theory corrections

Jianwen Jiang and John M. Prausnitz [*]

Department of Chemical Engineering, University of California, Berkeley, California 94720

and Chemical Sciences Division, Lawrence Berkeley National Laboratory, University of California, Berkeley, California 94720

Abstract

A recently developed crossover equation of state incorporates contributions from long-wavelength density fluctuations by renormalization-group theory. This equation of state can satisfactorily describe the thermodynamic properties of chain fluids both far-from and near-to the critical region; it is used here to calculate the critical locus of a mixture. Because the calculations require much computation time, especially for ternary (any higher) mixtures, an interpolation method is used as suggested by Redlich over 30 years ago. For a binary mixture, along the critical line that gives the critical temperature or critical pressure as a function of composition, the limiting slopes at the critical points of the pure components are explicitly derived from the criteria for a critical point. Logarithmic-hyperbolic interpolation equations are selected to calculate the entire critical line of the binary mixtures; this procedure is then generalized to multicomponent mixtures. Upon comparison with experimental critical data, the interpolation equations give good critical lines for binary and multicomponent Type I mixtures of *n*-alkanes.

Keywords: Critical point; Equation of state; Density fluctuation; Renormalization-group theory; *n*-Alkane mixtures

---

[*] Corresponding author. Tel: 510-642-3592; Fax: 510-642-4778; e-mail: lindar@cchem.berkeley.edu

1. Introduction

Since the early 1980s, industrial applications of supercritical fluids (SCF) have become useful for a number of processes, for example, for coffee decaffeination, production of natural-flavor and dyeing materials, separation of involatile mixtures, waste treatment [1] and fermentations [2]. Supercritical fluids are also useful for devolatilizing polymer solutions to remove unreacted monomers and polymerization solvents [3].

SCF can be used as reaction media [4,5] and as solvents in polymerization processes [6,7]. A mixture of SCF and specialty surfactants has been developed for dry cleaning and paint spraying [8]. Some of these industrial applications of SCF are attractive as promising "green" processes [8,9] that protect the natural environment.

Design of processes using SCF requires quantitative information of the critical loci of fluid mixtures. The critical locus defines the limiting condition where the system can exist in two coexisting phases; near the critical point, the density-dependent properties change dramatically with small changes in temperature or pressure.

Many studies are concerned with empirical correlations for critical properties [10–19] and several popular equations of states (EOS) like RK [20], SRK [21], PR [22] and SAFT [23-25] have been used to determine critical points. It has been long recognized, however, that although these EOSs can describe fluid properties fairly well far away from the critical point, because they are mean-field based, they cannot yield the correct limiting properties at the critical point. The mean-field theories assume that the immediate environment of each particle in a fluid has the same composition and density as those of the bulk fluid. Mean-field theories neglect density fluctuations that become large near the critical point [26]. A detailed historical review on the weaknesses and strengths of mean-field theories has been given by Levelt-Sengers [27].

Upon incorporation of contributions from long-wavelength density fluctuations by renormalization-group (RG) theory, we have developed [28] a crossover EOS for chain fluids (EOSCF+RG). This EOS correctly represents phase equilibria and pVT properties of pure chain fluids near-to and far-from the critical point. Good agreement is obtained upon comparison with computer simulations for square-well chain fluids and with experimental data for n-alkanes. It appears to be a promising EOS for describing thermodynamic properties of chain fluids both near-to and far-from the critical region. In this work, using this EOS, we calculate the critical points of hydrocarbon mixtures.

2. Critical-Point Calculations

The thermodynamic basis for critical-point calculation was provided by Gibbs [29]. For a multicomponent mixture, the critical point is obtain from two equations in the form of two determinants:

$$D_1 = \det \left| \frac{\partial^2 G}{\partial x_i \partial x_j} \right| = 0 \tag{1.a}$$

$$D_2 = \det \left| (1 - \delta_{ki}) \frac{\partial^2 G}{\partial x_i \partial x_j} + \delta_{ki} \frac{\partial D_1}{\partial x_j} \right| = 0 \tag{1.b}$$

where G is Gibbs energy; x_i is composition of component i; k is a fixed number; the difference between determinants D_2 and D_1 is that the kth column of D_1 is replaced by $\partial D_1 / \partial x_j$. Eqs. (1.a) and (1.b) can also be represented in terms of other thermodynamic variables [30].

The critical point can be determined by computational techniques for solving these two equations simultaneously, as discussed previously for binary and ternary systems [31–37], and for multicomponent mixtures [38–39]. These techniques, however, have to evaluate a large number of determinants and are computationally expensive, especially for mixtures with many components. To simplify the calculations, using a Taylor expansion of Helmholtz energy A, Heidemann and Khalil [40] use these criteria:

$$\sum_i \sum_j \frac{\partial^2 A}{\partial n_i \partial n_j} \Delta n_i \Delta n_j = 0 \tag{2.a}$$

$$\sum_i \sum_j \sum_k \frac{\partial^3 A}{\partial n_i \partial n_j \partial n_k} \Delta n_i \Delta n_j \Delta n_k = 0 \tag{2.b}$$

where $\Delta n_i = n_i - n_i^0$ is a small perturbation from the original state n_i^0; here n_i is the number of moles of components. This algorithm finds the critical state by nested one-dimensional iterations of the Newton-Raphson method, requires evaluation of only one determinant and avoids differentiation of determinants. The method of Heidemann and Khalil is reliable for critical-point calculations [41–42] and has also been used to calculate tricritical points [43]. Michelsen [44] used an alternate efficient technique that does not use any determinants but depends on an eigenvalue method. Another efficient algorithm was proposed by Hicks and Young [45] and extended by Sadus [46–47]; first, eq. (1.a) is solved separately and then D_2 is evaluated using the solution of eq. (1.a). This procedure is repeated until D_2 changes sign. The purpose is to guarantee that all roots are found.

All of these computational methods for critical-point calculation are mathematically effective but, in practice, they always use a mean-field EOS. Because a mean-field EOS cannot reproduce the global

phase behavior of fluids, it follows that, to obtain good results in the critical region, the adjustable parameters are different from those needed to obtain good results away from the critical region [34–36].

3. EOS with RG correction

The inability of mean-field theories to describe critical behavior was known many years ago but a method for corrections became available only relatively recently. Taking long-range density fluctuations into account, scaling and crossover theory can correct the mean-field theory [48–55]. The theory developed by Sengers et al. [51–53] and Kiselev et al. [54,55] incorporates a crossover from singular thermodynamic behavior at the critical point to regular thermodynamic behavior far away from the critical point. In this way the common engineering EOS can be used near the critical point and yield correct critical behavior. However, the physical meaning of the many crossover parameters is not clear in terms of molecular properties.

White and coworkers [56–58] developed a global renormalization-group (RG) theory based on the phase-space cell approximation; when extended beyond the range of the original RG theory, White's theory can be applied beyond the critical region. The few parameters in this theory have a molecular basis.

Lue and Prausnitz [59-60] extended the accuracy and range of White's RG transformation through an improved Hamiltonian. Good representations of thermodynamic properties and phase equilibria were obtained for square-well (SW) model fluids and their mixtures. Tang [61], and White and Zhang [62] have also studied the properties of Lennard-Jones fluids. However, these publications were directed to fluids containing simple spherical molecules although they were applied also to non-spherical molecules using a cubic EOS [63].

Based on the work of Lue and Prausnitz, we [28] developed a crossover EOS for pure chain fluids (EOSCF+RG) by incorporating of contributions from long-wavelength density fluctuations using RG theory. Outside the critical region, the crossover EOSCF+RG reduces to the classical EOS [23-25, 64-66]; inside the critical region, it gives non-classical universal critical exponents.

For a binary mixture, we model each fluid as a homosegmented chain with chain length m_1 or m_2, and segment diameter σ_1 or σ_2. Interaction between chain segments is given by a square-well (SW) potential:

$$u_{ij}(r) = \begin{cases} \infty & r < \sigma_{ij} \\ -\varepsilon_{ij} & \sigma_{ij} < r < \lambda_{ij}\sigma_{ij} \qquad (i,j=1,2) \\ 0 & r > \lambda_{ij}\sigma_{ij} \end{cases} \tag{3}$$

where σ_{ij} is an additive hard-sphere diameter given by

$$\sigma_{ij} = \frac{\sigma_i + \sigma_j}{2} \tag{4}$$

Parameters ε_{ij} and λ_{ij}, denoting the reduced width and depth of the SW interaction potential for pair ij, respectively, are related to those parameters for pure components by

$$\varepsilon_{ij} = \sqrt{\varepsilon_i \varepsilon_j}(1 - k_{ij}) \tag{5}$$

$$\lambda_{ij} = \frac{\lambda_i \sigma_i + \lambda_j \sigma_j}{\sigma_i + \sigma_j} \tag{6}$$

If the cross parameter k_{ij} is set to zero, equations (4) and (5) are the so-called Lorentz (energy)-Berthelot (size) approximation [67].

Without loss of generality, but with a view towards fitting experimental data, we assume that ε_i depends on temperature T as proposed by Chen and Kreglewski [68]

$$\varepsilon_i = \varepsilon_i^0 (1 + e/k_B T) \tag{7}$$

where k_B is Boltzmann's constant; e/k_B is a constant equal to 5K. Following Barker-Henderson (BH) theory [69–70], the temperature dependence of the effective diameter σ_i is

$$\sigma_i = \sigma_i^0 \left[1 - C\exp(-3\varepsilon_i^0 / k_B T) \right] \tag{8}$$

where σ_i^0 is a temperature-independent diameter. C is an integration constant; following Chen and Kreglewski [68], we set $C = 0.12$.

The Helmholtz energy density f, i.e., the Helmholtz energy per unit of volume V, is obtained from the general form of the EOSCF,

$$f^{\text{EOSCF}} = f^{\text{id}} + f^{\text{hs}} + f^{\text{sw}} + f^{\text{chain}}. \tag{9}$$

Contributions from ideal-gas, hard-sphere, attractive SW and chain formation are given explicitly in Appendix A.

5

The equations above constitute the EOSCF (without RG corrections) for a binary mixture. However, EOSCF performs well only far from the critical region where density fluctuations are very small. Following the work of White [56–58], and Lue and Prausnitz [59–60], incorporation of the contributions from density fluctuations with longer and longer wavelengths leads to EOSCF+RG. Recursion relations are used to evaluate the Helmholtz energy density (see ref. 28 for details):

$$f_n(\rho) = f_{n-1}(\rho) + \delta f_n(\rho) \tag{10}$$

$$\delta f_n(\rho) = -K_n \ln \frac{\Omega_n^s(\rho)}{\Omega_n^l(\rho)}, \qquad 0 \le \rho < \rho_{\max}/2 \tag{11.a}$$

$$\delta f_n(\rho) = 0, \qquad \rho_{\max}/2 \le \rho < \rho_{\max} \tag{11.b}$$

where Ω_n^l and Ω_n^s refer to density fluctuations for long-range attraction and for short-range attraction, respectively; $\rho_{\max}$ is the maximum possible number density, and

$$K_n = \frac{k_B T}{2^{3n} L^3} \tag{12}$$

$$\Omega_n^\alpha(\rho) = \int_0^{\rho_1} dz_1 \int_0^{\rho_2} dz_2 \exp[-\overline{E}_n^\alpha(\rho, z)/K_n], \qquad \alpha = s, l \tag{13}$$

$$2\overline{E}_n^\alpha(\rho, z) = \overline{f}_n^\alpha(\rho + z) + \overline{f}_n^\alpha(\rho - z) - 2\overline{f}_n^\alpha(\rho), \qquad \alpha = s, l \tag{14}$$

$$\overline{f}_n^l(\rho) = f_{n-1}(\rho) + \sum_{i=1}^{2} \sum_{j=1}^{2} b_{ij} \rho_i \rho_j \tag{15}$$

$$\overline{f}_n^s(\rho) = f_{n-1}(\rho) + \sum_{i=1}^{2} \sum_{j=1}^{2} b_{ij} \rho_i \rho_j \frac{\Phi_{ij} \xi_{ij}^2}{2^{2n+1} L_{ij}^2} . \tag{16}$$

where b_{ij} is the interaction volume and ξ_{ij} refers to the range of the attractive potential. They are related to the SW potential by

$$b_{ij} = \frac{2\pi}{3} \varepsilon_{ij} (\lambda_{ij} \sigma_{ij})^3 \tag{17}$$

$$\xi_{ij}^2 = \frac{1}{5} (\lambda_{ij} \sigma_{ij})^2 \tag{18}$$

Parameter L_{ij} is the cut-off length; we use the same L for all components. Φ_{ij} is the average gradient of the wavelet function, given by

$$\Phi_{ij} = \frac{\Phi_i \sigma_i + \Phi_j \sigma_j}{\sigma_i + \sigma_j} \tag{19}$$

The above recursion procedure can be interpreted as calculation of the ratio of non-mean-field contributions to mean-field contributions at gradually increasing long wavelengths. We perform the calculations numerically with a density step $6/(\pi m_i \sigma_i^3 500)$ for each component, and smooth the resulting Helmholtz energy density by a two-dimensional cubic spline function [74]. In principle, the recursion should be performed until index n approaches infinity; however, in our calculation we find that $n = 5$ is sufficient.

After we calculate the Helmholtz energy of the system, pressure is obtained by

$$P = -f + \rho \left(\frac{\partial f}{\partial \rho} \right)_{T,N} \tag{20}$$

where N is the total number of molecules.

In his review of the legacy of Otto Redlich [75], Prausnitz recalled that, if the effect of composition on the thermodynamic properties of a binary mixture can be determined at the boundary conditions ($x_1 = 0$ and $x_1 = 1$, where x is mole fraction), then an interpolation can be used to estimate properties at intermediate mole fractions. In the present work, we use Redlich's interpolation function to calculate the critical points of a mixture.

For a binary mixture, Redlich and coworkers [76–77] found that along the critical line, the limiting slopes at the critical points of two pure components can be explicitly derived from the critical criteria, as shown in Appendix B. They obtained fairly good results using classical EOS such as those by Redlich-Kwong and Benedict-Webb-Rubin. However, a classical phenomenological EOS is not suitable to describe critical points because they neglect density fluctuations. In the present work, we use EOSCF+RG. Following the work of Redlich, we adopt logarithmic-hyperbolic interpolation functions to estimate the critical temperatures and pressures for a binary mixture:

$$\ln T^c = x_1 \ln T_1^c + x_2 \ln T_2^c + \frac{(\ln T_1^c - \ln T_2^c - t_2/T_2^c)x_1(\ln T_1^c - \ln T_2^c - t_1/T_1^c)x_2}{(\ln T_1^c - \ln T_2^c - t_2/T_2^c)x_1 - (\ln T_1^c - \ln T_2^c - t_1/T_1^c)x_2} \tag{21}$$

$$\ln P^c = x_1 \ln P_1^c + x_2 \ln P_2^c + \frac{(\ln P_1^c - \ln P_2^c - p_2/P_2^c)x_1(\ln P_1^c - \ln P_2^c - p_1/P_1^c)x_2}{(\ln P_1^c - \ln P_2^c - p_2/P_2^c)x_1 - (\ln P_1^c - \ln P_2^c - p_1/P_1^c)x_2} \tag{22}$$

where T_i^c and P_i^c are the critical temperature and pressure, respectively, for pure component i; the composition of the mixture is given by mole fraction x_i. When T^c and P^c are plotted versus x_i, t_i and p_i are the limiting slopes of critical temperature and pressure, respectively, when $x_i = 1$ as shown in eqs. (B.12) and (B.13).

For a multicomponent mixture with M components, we propose the following interpolation equations:

$$\ln T^c = \sum_{i=1}^{M} x_i \ln T_i^c + \sum_{i=1}^{M-1} \sum_{j=i+1}^{M} (x_i + x_j) \frac{(\ln T_i^c - \ln T_j^c - t_j^{ij}/T_j^c)x_i(\ln T_i^c - \ln T_j^c - t_i^{ij}/T_i^c)x_j}{(\ln T_i^c - \ln T_j^c - t_j^{ij}/T_j^c)x_i - (\ln T_i^c - \ln T_j^c - t_i^{ij}/T_i^c)x_j} \tag{23}$$

$$\ln P^c = \sum_{i=1}^{M} x_i \ln P_i^c + \sum_{i=1}^{M-1} \sum_{j=i+1}^{M} (x_i + x_j) \frac{(\ln P_i^c - \ln P_j^c - p_j^{ij}/P_j^c)x_i(\ln P_i^c - \ln P_j^c - p_i^{ij}/P_i^c)x_j}{(\ln P_i^c - \ln P_j^c - p_j^{ij}/P_j^c)x_i - (\ln P_i^c - \ln P_j^c - p_i^{ij}/P_i^c)x_j} \tag{24}$$

where t_i^{ij} and p_i^{ij} are limiting slopes for binary mixture $i\text{-}j$. When $M = 2$, eqs. (23) and (24) reduce to eqs. (21) and (22), respectively.

4. Results and Discussion

4.1. Segment-Segment Parameters

To illustrate our procedure, we calculate the critical temperatures and pressures for n-alkane mixtures containing the major components of liquefied natural gas (LNG), i.e. methane, ethane, propane, n-butane, n-pentane and n-hexane.

The segment-segment parameters for each component have been correlated in our previous work [28]. The chain length of n-alkane is estimated from a simple empirical relation with carbon number C_i by $m_i = 1 + (C_i - 1)/3$. For each pure component, interaction potential ε_i^0, segment diameter σ_i^0 and interaction width λ_i are optimized to fit experimental data outside the critical region. To incorporate contributions from long-wavelength density fluctuations inside the critical region, we set the cut-off length $L = 11.5\,\text{Å}$ and select a suitable parameter Φ_i to fit the measured pure-component critical properties. Segment-segment parameters are given by Jiang and Prausnitz [28].

We fit cross parameter k_{ij} to measured vapor-liquid equilibrium data [81–82] outside the critical region for all binary pairs among methane, ethane, propane, n-butane, n-pentane and n-hexane. Table 1 shows the optimized k_{ij}. Parameter k_{ij} in a binary series rises with carbon number of the second component, as observed previously [83].

4.2. Critical Lines for Binary Mixtures

Fig.1(a) shows critical temperatures and pressures for binary mixtures of C_1–C_3 as a function of composition. Triangles denote the experimental critical temperatures [84]; circles refer to the experimental critical pressures [84]. Solid lines are calculated from the interpolation method based on

EOSCF+RG; dashed lines are calculated based on EOSCF. With increasing mole fraction of composition 1 (C_1), the critical temperature monotonically decreases; however, the critical pressure shows a maximum. While EOSCF+RG satisfactorily predicts the measured critical lines, EOSCF overestimates both critical temperatures and critical pressures. EOSCF+RG provides much improvement over EOSCF.

Fig.1(b) shows P-T loci for binary mixtures of C_1–C_3. The left line is for pure C_1; the right line is for pure C_3; points C_1 and C_3 are critical points of the two pure components; the line connecting C_1 and C_3 gives critical points for the mixture. Squares are experimental data [84]; diamonds are critical points of pure C_1 and C_3 calculated from EOSCF; solid lines are calculated from EOSCF+RG and the dashed lines are from EOSCF. There is a maximum in the continuous C_1–C_3 line; this system belongs to Type I as characterized by Scott and Konynenburg [85–87]. EOSCF+RG gives results consistent with experimental data. The need for RG corrections is evident.

Fig.2 and 3 show critical lines for C_2–n-C_4 and for n-C_4–n-C_6 binary mixtures, respectively. Results are similar to those shown in Fig. 1 for C_1–C_3.

4.3. Critical Properties for Multicomponent Mixtures

To test our interpolation method by comparison with experiment, we calculate the critical temperatures and pressures for 23 multicomponent mixtures composed of methane, ethane, propane, n-butane, n-pentane or n-hexane. Table 2 gives the composition of each mixture. Table 3 gives the measured critical temperatures and pressures [88–93], and those calculated using EOSCF+RG and interpolations as indicated in eqs. (23) and (24). Calculated results agree well with experiment, especially if we consider probable experimental uncertainties in critical pressures.

5. Conclusion

The interpolation method proposed by Redlich et al to predict the critical properties of Type 1 or Type 2 binary mixtures is extended to multicomponent mixtures. Using a recently developed equation of state for chain fluids with renormalization-group-theory corrections (EOSCF+RG), the interpolation method gives critical temperatures and pressures in good agreement with experimental data for mixtures of n-alkanes.

Because renormalization-group theory corrections require extensive computations, the calculations for critical temperatures and pressures described here are more complex than those using conventional methods with a classical equation of state. The latter often give good results because they use experimental critical temperatures and pressures for pure components as input parameters and, in at least

some cases, because they use binary parameters (k_{ij}) to fit experimental critical temperatures and pressures for binary mixtures.

By contrast, the method described here uses adjustable binary parameters obtained only from binary data far removed from critical conditions. In other words, the method discussed here is predictive because, unlike those based on classical equation of state, in this RG-corrected work, the important role of density fluctuations in the critical region is taken into account.

For typical contemporary practical engineering work, the classical methods are probably sufficient. But for cases when a more detailed description of critical phenomena is required, it will be necessary to replace a classical equation of state with one that includes RG corrections.

6. List of symbols

b_{ij}	interaction volume for ij
A	Helmholtz energy
C	integration constant in BH theory
D_i	determinant value in criteria for critical point ($i = 1, 2$)
f	Helmholtz energy density
$g_{ij}(r)$	pair correlation function
G	Gibbs energy
k_B	Boltzmann constant
k_{ij}	cross parameter for binary mixture ij
L	cut-off length
m_i	chain length of molecule i
M	number of components
n_i	mole number of component i
N	total number of molecules
P	pressure
P^c	critical pressure of mixture
P_i^c	critical pressure of component i
p_i	limiting slope of critical-pressure line for a binary mixture when $x_i = 1$

r	center-to-center distance
SW	square-well potential
T^c	critical temperature of mixture
T_i^c	critical temperature of component i
t_i	limiting slope of critical temperature for a binary mixture when $x_i = 1$
u	interaction potential
V	total volume of the system
$\bar{V_i}$	partial molar volume of component i
x_i	mole fraction of component i
$y_{ij}(r)$	cavity correlation function

Greek letters

ρ_i	number density of molecule i
σ_i	segment diameter of molecule i
ε_i	SW interaction well-depth of molecule i
λ_i	SW interaction range of molecule i
Λ_i	de Broglie thermal wavelength of molecule i
ϕ_i	fugacity coefficient of component i
μ_i	chemical potential of component i
Φ_i	average gradient of wavelet function for component i

Superscripts

c	critical point
l	long wavelength
s	short wavelength

Subscript

i	component i

7. Literatures Cited

[1] K. Arai, Simulation, Material Conversation, and Chemistry of Supercritical Water Systems, 4th International Symposium on Supercritical Fluids, Sendai, Japan, May (1997).

[2] C. E. Fabre, J.-S. Condoret, A. Marty, Extractive Fermentation of Aroma with Supercritical CO2, Biotech. & Bioeng. 64 (1999) 392–400.

[3] H. Inomata, Y. Honma, M. Imahori, K. Arai, Fundamental Study of de-Solventing Polymer Solutions with Supercritical CO_2, Fluid Phase Equilibria, 158-160 (1999) 857–867.

[4] J. F. Brennecke, Green Processing Using Ionic Liquids and CO_2, Nature, 399 (1999) 28–29.

[5] D. P. Roek, M. J. Kremer, C. B. Roberts, J. E. Chateauueuf, J. F. Brennecke, Spectroscopic Studies of Solvent Effects on Reactions in Supercritical Fluids, Fluid Phase Equilibria, 158–160 (1999) 713–722.

[6] K. F. Webb, A. S. Teja, Solubility and Diffusion of Carbon Dioxide in Polymers, Fluid Phase Equilibria, 158-160 (1999) 1029–1034.

[7] Supercritical CO_2 Route to Teflon Will Get an Industrial-Scale Tryout, Chem. Eng. May (1999) 17.

[8] Process Uses Ionic Liquid and CO_2, C&EN, May 10 (1999) 9.

[9] Industry Intrigued by CO_2 as Solvent, C&EN, June 14 (1999) 11.

[10] F. Kurata, D. K. Katz, Critical Properties of Volatile Hydrocarbon Mixtures, Trans. Am. Inst.Chem. Engrs. 38 (1942) 995–1021.

[11] C. K. Eilerts, et al., *Phase Relations of Gas-Condensate Fluids, Vol. 1, Monograph No. 10*, U.S. Bureau of Mines, 1957.

[12] R. B. Grieves, G. Thodos, The Critical Temperatures and Pressures of Binary Systems: Hydrocarbons of All Types and Hydrogen, AIChE J. 6 (1960) 561–566.

[13] R. B. Grieves, G. Thodos, The Critical Temperatures of Multicomponent Hydrocarbon Systems, AIChE J. 8 (1962) 550–553.

[14] R. B. Grieves, G. Thodos, The Critical Pressures of Multicomponent Hydrocarbon Mixtures and the Critical Densities of Binary Hydrocarbon Mixtures, AIChE J. 9 (1963) 25–30.

[15] D. O. Etter, W. B. Kay, Critical Properties of Mixtures of Normal Paraffin Hydrocarbons, J. Chem. Eng. Data, 6 (1961) 409–414.

[16] P. L. Chueh, J. M. Prausnitz, Vapor-Liquid Equilibria at High Pressures: Calculation of Critical Temperatures, Volumes, and Pressures of Nonpolar Mixtures, AIChE J. 13 (1967) 1107–1113.

[17] A. Kreglewski, W. B. Kay, The Critical Constants of Conformal Mixtures, J. Phys. Chem. 73 (1969) 3359–33.

[18] C. C. Li, Critical Temperature Estimation for Simple Mixtures, Can. J. Chem. Eng. 49 (1971) 709–710.

[19] C. F. Spencer, T. E. Daubert, R. P. Danner, A Critical Review of Correlations for the Critical Properties of Defined Mixtures, AIChE J. 19 (1973) 522–526.

[20] O. Redlich, J. N. S. Kwong, On the Thermodynamics of Solutions. V An Equation of State. Fugacities of Gaseous Solutions, Chem. Rev. 44 (1949) 233–244.

[21] G. Soave, Equilibrium Constants from a Modified Redlich-Kwong Equation of State, Chem. Eng. Sci. 27 (1972) 1197–1203.

[22] D. Peng, D. B. Robinson, A New Two-Constant Equation of State, Ind. Eng. Chem. Fundam. 15 (1976) 59–64.

[23] W. G. Chapman, K. E. Gubbins, G. Jackson, M. Radosz, New Reference Equation of State for Associating Liquids, Ind. Eng. Chem. Res. 29 (1990) 1709–1721.

[24] S. H. Huang and M. Radosz, Equation of State for Small, Large, Polydisperse and Associating Molecules, Ind. Eng. Chem. Res. 29 (1990) 2284–2294.

[25] S. H. Huang and M. Radosz, Equation of State for Small, Large, Polydisperse and Associating Molecules: Extension to Fluid Mixtures, Ind. Eng. Chem. Res. 30 (1991) 1994–2005.

[26] M. E. Fisher, Renormalization Group Theory: Its Basis and Formulation in Statistical Physics, Rev. Mod. Phys., 70 (1998), 653–681.

[27] J. M. H. Levelt Sengers, Mean-Field Theories, Their Weaknesses and Strength, Fluid Phase Equil. 158/160 (1999) 3–17.

[28] J. Jiang, J. M. Prausnitz, Equation of State for Thermodynamic Properties of Chain Fluids Near-to and Far-from the Vapor-Liquid Critical Region, J. Chem. Phys. 111 (1999), in press.

[29] J. W. Gibbs, On the Equilibrium of Heterogeneous Substances (Oct. 1876-May 1877), *The Collected Works of J. Willard Gibbs, Vol. 1, Thermodynamics,* Yale University Press, New Haven, CN, 1928.

[30] J. W. Tester, M. Modell, *Thermodynamics and its applications*, 3rd Ed., Prentice-Hall Inc., NJ, 1996.

[31] R. R. Spear, R. L. Robinson Jr., K. C. Chao, Critical States of Mixtures and Equations of State, Ind. & Eng. Chem. Fund. 8 (1969) 2–7.

[32] R. R. Spear, R. L. Robinson Jr., K. C. Chao, Critical States of Ternary Mixtures and Equations of State, Ind. & Eng. Chem. Fund. 10 (1971) 588–592.

[33] A. S. Teja, J. S. Rowlinson, The Prediction of the Thermodynamic Properties of Fluids and Fluid Mixtures–IV. Critical and Azeotropic States, Chem. Eng. Sci. 28 (1973) 529–538.

[34] A. Galindo, P. J. Whitehead, G. Jackson, A. N. Burgess, Predicting the High-Pressure Phase Equilibria of Water+n-Alkanes Using a Simplified SAFT Theory with Transferable Intermolecular Interaction Parameters, J. Phys. Chem. 100 (1996) 6781–6792.

[35] C. McCabe, G. Jackson, SAFT-VR Modelling of the Phase Equilibrium of Long-Chain n-Alkanes, Phys. Chem. Chem. Phys. 1 (1999) 2057–2064.

13

[36] F. J. Blas, L. F. Vega, Critical Behavior and Partial Miscibility Phenomena in Binary Mixtures of Hydrocarbons by the Statistical Associating Fluid Theory, J. Chem. Phys. 109 (1998) 7405–7413.

[37] H. Adidharma, M. Radosz, Prototype of an Engineering Equation of State for Heterosegmented Polymers, Ind. Eng. Chem. Res. 37 (1998) 4453–4462.

[38] D. Y. Peng, D. B. Robinson, A Rigorous Method for Predicting the Critical Properties of Multicomponent Systems from an Equation of State, AIChE J. 23 (1977) 137–144.

[39] L. E. Baker, K. D. Luks, Critical Point and Saturation Pressure Calculations for Multicomponent Systems, Soc. Petro. Engrs. J. 20 (1980) 15–24.

[40] R. A. Heidemann, A. M. Khalil, The Calculation of Critical Points, AIChE J. 26 (1980) 769–779.

[41] G. N. Charos, P. Clancy, K. Gubbins, C. D. Naik, Three-Dimensional PTx Phase Diagrams Through Interactive Computer Graphics, Fluid Phase Equili. 23 (1985) 59–78.

[42] S. I. Abu-Eishah, Modification of the Predictive Capability of the PRSV-2 Equation of State for Critical Volumes of Binary Mixtures, Fluid Phase Equili. 157 (1999) 1–16.

[43] B. F. Kohse, R. A. Heidemann, Computation of Tricritical Points in Ternary Systems, AIChE J. 39 (1993) 1242–1256.

[44] M. L. Michelsen, Calculation of Critical Points and Phase Boundaries in the Critical Region, Fluid Phase Equili. 16 (1984) 57–76.

[45] C. P. Hicks, C. L. Young, J. Chem. Soc. Faraday Trans. II, 73 (1977) 597–612.

[46] R. J. Sadus, *High Pressure Phase Behavior of Multicomponent Fluid Mixtures*, Elsevier Sci., Netherlands, 1992.

[47] R. J. Sadus, Calculating Critical Transitions of Fluid Mixtures–Theory vs. Experiment, AIChE J. 40 (1994) 1376–1403, and references therein.

[48] J. J. de Pablo, J. M. Prausnitz, Liquid-Liquid Equilibria for Binary and Ternary Systems Including the Critical Region. Transformation to Non-Classical Coordinates, Fluid Phase Equil. 50 (1989) 101–131.

[49] J. J. de Pablo, J. M. Prausnitz, Thermodynamics of Liquid-Liquid Equilibria Including the Critical Region. Transformation to Non-Classical Coordinates Using Revised Scaling, Fluid Phase Equil. 59 (1990) 1–14.

[50] D. H. Smith, J. J. Lynch, Modeling of Fluid Phase Equilibrium of Multicomponent Hydrocarbon Mixtures in the Critical Region, Fluid Phase Equil. 98 (1994) 35–48.

[51] M. A. Anisimov S. B. Kiselev, J. V. Sengers, S. Tang, Crossover Approach to Global Critical Phenomena in Fluids, Physica A, 188 (1992) 487–525.

[52] M. A. Anisimov, A. A. Povodyrev, J. V. Sengers, Crossover Critical Phenomena in Complex Fluids, Fluid Phase Equil. 158 (1999) 537–547.

[53] T. A. Edison, J. V. Sengers, Thermodynamic Properties of Ammonia in the Critical Region, Int. J. Refrig. 22 (1999) 365–378.

[54] S. B. Kiselev, Cubic Crossover Equation of State, Fluid Phase Equil. 147 (1998) 7–23.

[55] S. B. Kiselev, D. G. Friend, Cubic Crossover Equation of State for Mixtures, Fluid Phase Equil. 162 (1999) 51–82.

[56] J. A. White, Contribution of Fluctuations to Thermal Properties of Fluids with Attractive Forces of Limited Range: Theory Compared with $P \rho T$ and C_V Data for Argon, Fluid Phase Equil. 75 (1992) 53–64.

[57] J. A. White, S. Zhang, Renormalization Group Theory for Fluids, J. Chem. Phys. 99 (1993) 2012–2019.

[58] J. A. White, S. Zhang, Renormalization Group Theory for Fluids to Greater Density Distances from the Critical Point, Int. J. Thermophys. **19**, 1019–1027 (1998)

[59] L. Lue, J. M. Prausnitz, Renormalization-Group Theory Corrections to an Approximation Free-Energy Model for Simple Fluids Near to and Far from the Critical Region, J. Chem. Phys. 108 (1998) 5529–5536.

[60] L. Lue, J. M. Prausnitz, Thermodynamics of Fluid Mixtures Near to and Far from the Critical Region, AIChE J. 44 (1998) 1455–1466.

[61] Y. Tang, Outside and Inside the Critical Region of the Lennard-Jones Fluid, J. Chem. Phys. 109 (1998) 5935–5944.

[62] J. White, S. Zhang. Lennard-Jones as a Model for Argon and Test of Extended RG Calculations, J. Chem. Phys. (1999) in press.

[63] F. Fornasiero, L. Lue, A. Bertucco, Improving Cubic EOSs Near the Critical Point by a Phase-Space Cell Approximation, AIChE J. 45 (1999) 906–915.

[64] Y. Hu, H. Liu, J. M. Prausnitz, Equation of State for Fluids Containing Chainlike Molecules, J. Chem. Phys. 104 (1996) 396–404.

[65] H. Liu, Y. Hu, Equation of State for Systems Containing Chainlike Molecules, Ind. Eng. Chem. Res. 37 (1998) 3058–3066.

[66] J. Jiang, H. Liu, Y. Hu, J. M. Prausnitz, A Molecular-Thermodynamic Model for Polyelectrolyte Solutions, J. Chem. Phys. 108 (1998) 780–784.

[67] J. S. Rowlinson, F. L. Swinton, *Liquids and Liquid Mixtures*, 3rd ed., Butterworths, London ,1982.

[68] S. S. Chen, A. Kreglewski, Applications of the Augmented van der Waals Theory of Fluids. I. Pure Fluids, Ber. Bunsen-Ges. Phys. Chem. 81 (1977) 1048.

[69] J. A. Barker, D. Henderson, Perturbation Theory and Equation of State for Fluids: The Square Well Potential, J. Chem. Phys. 47 (1967) 2856–2861.

[70] J. A. Barker, D. Henderson, Perturbation Theory and Equation of State for Fluids: II. A Successful Theory of Fluids, J. Chem. Phys. 47 (1967) 4714–4721.

[71] T. Boublik, Hard-Sphere Equation of State, J. Chem. Phys. 53 (1970) 471–474.

[72] G. A. Mansoori, N. F. Carnahan, K. E. Starling, T. W. Leland, Equilibrium Thermodynamic Properties of the Mixture of Hard Spheres, J. Chem. Phys. 54 (1971) 1523–1525.

[73] A. Gil-Villegas, A. Galindo, P. J. Whitehead, S. J. Mills, G. Jackson, A. N. Burgess, Statistical Associating Fluid Theory for Chain Molecules with Attractive Potentials of Variable Range, J. Chem. Phys. 106 (1997) 4168–4186.

[74] W. H. Press, S. A. Teukolsky, W. T. Vetterling, B. P. Flannery, *Numerical Recipes in FORTRAN 77: The Art of Scientific Computing*, 2nd ed., Cambridge University Press, New York, 1992.

[75] J. M. Prausnitz, Equations of State from van der Waals Theory: The Legacy of Otto Redlich, Fluid Phase Equil. 24 (1985) 63–76.

[76] O. Redlich, A. T. Kister, On the Thermodynamics of Solutions: VII. Critical Properties of Mixtures, J. Chem. Phys. 36 (1962) 2002–2009.

[77] F. J. Ackerman, O. Redlich, On the Thermodynamics of Solutions: IX. Critical Properties of Mixtures and the Equation of Benedict, Webb, and Rubin, J. Chem. Phys. 38 (1963) 2740–2742.

[78] I. R. Krichevskii, Thermodynamics of Critical Phenomena in Infinitely Dilute Binary Solutions, Russ. J. Phys. Chem. 41 (1967) 1332–1338.

[79] J. M. H. Levelt Sengers, Dilute Mixtures and Solutions near Critical Points, Fluid Phase Equili. 30 (1986) 31–39.

[80] D. W. Jennings, M. T. Gude, A. S. Teja, High-Pressure Vapor-Liquid Equilibria in Carbon Dioxide and 1-Alkanol Mixtures, *Supercritical Fluid Engineering Science: Fundamentals and Applications*, E. Kiran, J. F. Brennecke, ed., Washington, DC, American Chemical Society, 1993.

[81] H. Knapp, R. Döring, L. Oellrich, U. Plöcker, J. M. Prausnitz, *Vapor-Liquid Equilibria for Mixtures of Low Boiling Substances*, Chemistry Data Series, Vol. VI, DECHEMA, 1982.

[82] W. B. Kay, R. L. Hoffman, O. Davis, Vapor-Liquid Equilibrium Relationship of Binary Systems *n*-Butane–*n*-Pentane and *n*-Butane–*n*-Hexane, J. Chem. Eng. Data 20 (1975) 333–338.

[83] M. D. Donohue, J. M. Prausnitz, Perturbed Hard Chain Theory for Fluid Mixtures: Thermodynamic Properties for Mixtures in Natural Gas and Petroleum Technology, AIChE J. 24 (1978) 849-860.

[84] C. P. Hicks, C. L. Young, The Gas-Liquid Critical Properties of Binary Mixtures, Chem. Rev. 75 (1975) 119–175.

[85] R. L. Scott, P. H. van Konynenburg, Static Properties of Solutions. Van der Waals and Related Models for Hydrocarbon Mixtures, Discuss. Faraday Soc. 49 (1970) 87.

[86] R. L. Scott, The Thermodynamics of Critical Phenomena in Fluid Mixtures, Ber. Bunsen-Ges. Phys. Chem. 76 (1972) 296–308.

[87] P. H. van Konynenburg, R. L. Scott, Philos. Trans. R. Soc. London, Ser. A 298 (1980) 495.

[88] G. W. Billman, B. H. Sage, W. N. Lacey, Phase Behavior in the Methane-Ethane-Pentane System, Trans. Am. Inst. Mining Met. Engrs. 174 (1948) 13.

[89] H. M. Cota, G. Thodos, Critical Temperatures and Critical Pressures of Hydrocarbon Mixtures, J. Chem. Eng. Data 7 (1962) 62–65.

[90] J. M. Nelson, D. E. Holcomb, Chem. Eng. Prog. Symp. Ser. 49 (1953) 93.

[91] A. R. Price, R. Kobayashi, Low Temperature Vapor-Liquid Equilibrium in Light Hydrocarbon Mixtures: Methane-Ethane-Propane System, J. Chem. Eng. Data 4 (1959) 40–52.

[92] P. Uchytil, I. Wichterle, Liquid-Vapor Critical Region of the Most Volatile Component of A Ternary System. I. Vapor-Liquid Equilibrium in the Ethane-Propane-n-Butane System, Fluid Phase Equil. 15 (1983) 209–217.

[93] L. Yarborough, L. R. Smith, Solvent and Driving Gas Compositions for Miscible Slug Displacement, Soc. Petrol. Eng. J. 10 (1970) 298.

Acknowledgements

Appendix A   Helmholtz energy for a binary mixture

There are four contributions to the Helmholtz energy.

$$f^{\text{EOSCF}} = f^{\text{id}} + f^{\text{hs}} + f^{\text{sw}} + f^{\text{chain}} \tag{A.1}$$

The contribution from the ideal gas is

$$f^{\text{id}} = k_{\text{B}} T \sum_{i=1}^{2} [\rho_i \ln(\rho_i \Lambda_i^3) - \rho_i] \tag{A.2}$$

where ρ_i is the number density for component i; and Λ_i denotes the de Broglie thermal wavelength of molecule i.

The hard-sphere interaction is given by Boublik and Mansoori et al, the so-called BMCSL equation [71–72]

$$f^{\text{hs}} = k_{\text{B}} T \left[(\zeta_2^3 / \zeta_3^2 - \zeta_0) \ln \Delta + \frac{\pi \zeta_1 \zeta_2 / 2 - \zeta_2^3 / \zeta_3^2}{\Delta} + \frac{\zeta_2^3 / \zeta_3^2}{\Delta^2} \right] \tag{A.3}$$

where $\zeta_n = \sum_{i=1}^{2} m_i \rho_i \sigma_i^n$ and $\Delta = 1 - \pi \zeta_3 / 6$.

The contribution from the SW attractive potential is estimated by the second-order Baker-Henderson perturbation theory [69–70]

$$f^{\text{sw}} = \frac{1}{\zeta_0} \sum_{i=1}^{2} \sum_{j=1}^{2} m_i m_j \rho_i \rho_j (a_1^{ij} + a_2^{ij} / k_{\text{B}} T). \tag{A.4}$$

The mean-attractive energy a_1^{ij} is given by a compact expression from the mean-value theorem [73]

$$a_1^{ij} = -2/3 \pi \zeta_0 \sigma_{ij}^3 \varepsilon_{ij} (\lambda_{ij}^3 - 1) g_{ij}^{\text{hs}} (\sigma_{ij}, \zeta_3^{\text{eff}}) \tag{A.5}$$

where the pair correlation function of hard-spheres at contact is evaluated at an effective ζ_3^{eff},

$$g_{ij}^{\text{hs}} (\sigma_{ij}) = \frac{1}{\Delta} + \frac{\pi \sigma_i \sigma_j \zeta_2}{4 \Delta^2 \sigma_{ij}} + \frac{\pi^2 \sigma_i^2 \sigma_j^2 \zeta_2^2}{72 \Delta^3 \sigma_{ij}^2} \tag{A.6}$$

with

$$\zeta_3^{\text{eff}} = c_1 \zeta_3 + c_2 \zeta_3^2 + c_3 \zeta_3^3. \tag{A.7}$$

Coefficients c_n are calculated by the matrix [73]

$$\begin{pmatrix} c_1 \\ c_2 \\ c_3 \end{pmatrix} = \begin{pmatrix} 2.25855 & -1.50349 & 0.249434 \\ -0.669270 & 1.40049 & -0.827739 \\ 10.1576 & -15.0427 & 5.30827 \end{pmatrix} \begin{pmatrix} 1 \\ \lambda_{ij} \\ \lambda_{ij}^2 \end{pmatrix} \tag{A.8}$$

The second perturbation term a_2^{ij} describing fluctuations of the attractive energy is given by

$$a_2^{ij} = \frac{\varepsilon_{ij}\zeta_0^2 \Delta^4}{2(\zeta_0 \Delta^2 + \pi\zeta_1\zeta_2\Delta + \pi^2\zeta_2^3/4)} \frac{\partial a_1}{\partial \zeta_0}.$$ (A.9)

The contribution from chain formation is

$$f^{chain} = k_B T \sum_{i=1}^{2} \rho_i (1-m_i) \ln y_{ii}^{sw}(\sigma_i).$$ (A.10)

where cavity correlation function $y_{ij}^{sw}(\sigma_{ij})$ at contact is defined by

$$y_{ij}^{sw}(\sigma_{ij}) = g_{ij}^{sw}(\sigma_{ij}) \exp(-\varepsilon_{ij}/k_B T)$$ (A.11)

with

$$g_{ij}^{sw}(\sigma_{ij}) = g_{ij}^{hs}(\sigma_{ij}) + \frac{1}{2\pi k_B T \sigma_{ij}^3} \left(3\frac{\partial a_1^{ij}}{\partial \zeta_0} - \frac{\lambda_{ij}}{\zeta_0}\frac{\partial a_1^{ij}}{\partial \lambda_{ij}} \right).$$ (A.12)

Appendix B   Critical line for a binary mixture

The critical criteria for a binary mixture may be expressed by

$$\left(\frac{\partial \mu_1}{\partial x_1}\right)_{T,P} = 0 \tag{B.1.a}$$

$$\left(\frac{\partial^2 \mu_1}{\partial x_1^{2}}\right)_{T,P} = 0 \tag{B.1.b}$$

where μ_1 is the chemical potential of component 1 whose mole fraction is x_1. According to the relation between chemical potential and fugacity, we have,

$$\left(\frac{\partial \ln \phi_1}{\partial x_1}\right)_{T,P} = -\frac{1}{x_1} \tag{B.2.a}$$

$$\left(\frac{\partial^2 \ln \phi_1}{\partial x_1^{2}}\right)_{T,P} = \frac{1}{x_1^{2}} \tag{B.2.b}$$

where ϕ_1 is the fugacity coefficient. Similar equations can also be written for component 2. Then

$$\left(\frac{\partial \ln(\phi_1 / \phi_2)}{\partial x_1}\right)_{T,P} = -\frac{1}{x_1 x_2} \tag{B.3.a}$$

$$\left(\frac{\partial^2 \ln(\phi_1 / \phi_2)}{\partial x_1^{2}}\right)_{T,P} = \frac{x_2 - x_1}{x_1^{2} x_2^{2}} \,. \tag{B.3.b}$$

On the other hand, the fugacity coefficient is defined using the partial molar volume by

$$\ln \phi_1 = \int_0^P (\overline{V}_1 / RT - 1/P)\, dP \tag{B.4}$$

Introducing the Gibbs-Duhem equation,

$$\overline{V}_1 - \overline{V}_2 = (\partial V / \partial x_1)_{T,P} \,, \tag{B.5}$$

we have

$$\ln(\phi_1 / \phi_2) = \int_0^P \left[(\partial V / \partial x_1)_{T,P} / RT\right] dP \,. \tag{B.6}$$

Eq. (6) transforms into

$$\ln(\phi_1 / \phi_2) = -\int_\infty^V \left[(\partial P / \partial x_1)_{T,V} / RT\right] dV \tag{B.7}$$

substitution of eq. (B.3.a) into the derivative of eq. (B.7) with respect to x_1, leads to

$$\int_{\infty}^{V}(\partial^2 P/\partial x_1^{\,2})_{T,V}\,dV - \int_{\infty}^{V}(\partial^2 P/\partial x_1 \partial V)_T\,(\partial V/\partial P)_{T,x_1}\,(\partial P/\partial x_1)_{T,V}\,\partial V$$
$$- (\partial P/\partial x_1)^2{}_{T,V}\,(\partial V/\partial P)_{T,x_1} = RT/x_1 x_2 \tag{B.8}$$

At the critical point of a pure component, i.e., $x_1 = 1$ or $x_1 = 0$, because $(\partial P/\partial V)_{T,x_1} = 0$, we obtain

$$(\partial P/\partial x_1)^2{}_{T,V} = -RT\lim_{x_1}[(\partial P/\partial V)_{T,x_1}/x_1 x_2] \tag{B.9}$$

For a mixture, along the critical line indicated by c,

$$[\partial(\partial P/\partial V)_{T,x_1}/\partial x_1]_c = (\partial^2 P/\partial V\partial x_1)_T + (\partial^2 P/\partial T\partial V)_{x_1}(\partial T/\partial x_1)_c$$
$$+ (\partial^2 P/\partial V^2)_{T,x_1}(\partial V/\partial x_1)_c \tag{B.10}$$

Combining eq. (B.10) with $(\partial^2 P/\partial V^2)_{T,x_1} = 0$ at the critical point of a pure component, we can derive the limit in the right side of eq. (B.9) as,

$$\lim_{x_1}[(\partial P/\partial V)_{T,x_1}/x_1 x_2] = [(\partial^2 P/\partial V\partial x_1)_T + (\partial^2 P/\partial T\partial V)_{x_1}(\partial T/\partial x_1)_c]/(x_2 - x_1) \tag{B.11}$$

where $x_1 \to 0$ or $x_1 \to 1$.

Eq. (B.9) can be rearranged into an explicit expression at the critical point of pure component 1 or 2:

$$t_1 = \lim_{x_1 \to 1}\left(\frac{\partial T}{\partial x_1}\right)_c = \lim_{x_1 \to 1}\left[\frac{(\partial P/\partial x_1)^2{}_{T,V}/RT - (\partial^2 P/\partial V\partial x_1)_T}{(\partial^2 P/\partial T\partial V)_{x_1}}\right] \tag{B.12.a}$$

$$t_2 = \lim_{x_1 \to 0}\left(\frac{\partial T}{\partial x_1}\right)_c = \lim_{x_1 \to 0}\left[\frac{-(\partial P/\partial x_1)^2{}_{T,V}/RT - (\partial^2 P/\partial V\partial x_1)_T}{(\partial^2 P/\partial T\partial V)_{x_1}}\right] \tag{B.12.b}$$

For slope of the critical-pressure line $(\partial P/\partial x_1)_c$, we have

$$p_1 = \lim_{x_1 \to 1}\left(\frac{\partial P}{\partial x_1}\right)_c = \lim_{x_1 \to 1}\left[(\partial P/\partial x_1)_{T,V} + t_1(\partial P/\partial T)_{V,x_1}\right] \tag{B.13.a}$$

$$p_2 = \lim_{x_1 \to 0}\left(\frac{\partial P}{\partial x_1}\right)_c = \lim_{x_1 \to 0}\left[(\partial P/\partial x_1)_{T,V} + t_2(\partial P/\partial T)_{V,x_1}\right] \tag{B.13.b}$$

Eqs. (B.12) and (B.13) give the limiting slopes at the ends of the critical lines for a binary mixture. Similar relations were used previously [78–80].

Table 1

Parameters k_{ij} for binary mixtures in this study [+]

	CH_4	C_2H_6	C_3H_8	$n\text{-}C_4H_{10}$	$n\text{-}C_5H_{12}$	$n\text{-}C_6H_{14}$
CH_4	0					
C_2H_6	0.0048	0				
C_3H_8	0.0150	0.0095	0			
$n\text{-}C_4H_{10}$	0.0255	0.0163	0.0040	0		
$n\text{-}C_5H_{12}$	0.0381	0.0220	0.0085	0.0029*	0	
$n\text{-}C_6H_{14}$	0.0490	0.0263	0.0131	0.0049	0	0

+: Data sources from Knapp et al. (1982). * from Knapp et al. (1982) and Kay et al. (1975).

Table 2

Compositions of multicomponent mixtures in this study

Mix. No.	CH_4	C_2H_6	C_3H_8	$n\text{-}C_4H_{10}$	$n\text{-}C_5H_{12}$	$n\text{-}C_6H_{14}$	Data sources
1	0.833	0.130	0.035				Price and Kobayashi (1959)
2	0.800	0.039	0.161				Price and Kobayashi (1959)
3[⊥]	0.4345	0.0835	0.4330				Yarborough and Smith (1970)
4	0.193	0.470		0.337			Cota and Thodos (1962)
5	0.391	0.354		0.255			Cota and Thodos (1962)
6	0.040	0.821		0.139			Cota and Thodos (1962)
7	0.007	0.879		0.114			Cota and Thodos (1962)
8	0.461	0.443			0.095		Billman et al. (1948)
9	0.196	0.758			0.045		Billman et al. (1948)
10		0.996	0.001	0.003			Uchytil and Wichterle (1983)
11		0.990	0.004	0.006			Uchytil and Wichterle (1983)
12		0.980	0.016	0.004			Uchytil and Wichterle (1983)
13		0.970	0.027	0.003			Uchytil and Wichterle (1983)
14		0.3414	0.3421		0.3165		Etter and Kay (1961)
15			0.3276	0.3398	0.3326		Etter and Kay (1961)
16			0.201	0.399	0.400		Nelson and Holcomb (1953)
17			0.201	0.298	0.501		Nelson and Holcomb (1953)
18			0.198	0.106	0.696		Nelson and Holcomb (1953)
19				0.6449	0.2359	0.1192	Etter and Kay (1961)
20		0.2542	0.2547	0.2554	0.2357		Etter and Kay (1961)
21			0.4858	0.3316	0.1213	0.0613	Etter and Kay (1961)
22	0.2019	0.2029	0.2033	0.2038	0.1881		Etter and Kay (1961)
23		0.3977	0.2926	0.1997	0.0713	0.0369	Etter and Kay (1961)

⊥: Mixture also contains a small amount of nitrogen.

23

Table 3

Experimental and calculated critical temperatures and pressures

Mixture	T^c(K)			P^c(MPa)		
	Exp.	Cal.	Dev. %	Exp.	Cal.	Dev. %
1	227.6	230.8	1.43	6.89	7.20	4.50
2	255.4	260.6	2.03	8.96	9.43	5.25
3	313.7	321.7	2.55	8.96	8.87	-1.00
4	354.3	350.7	-0.99	7.64	7.21	-5.63
5	331.5	333.3	0.53	9.72	9.49	-2.37
6	323.7	328.4	1.46	5.79	5.83	0.69
7	324.5	326.4	0.63	5.48	5.57	1.64
8	310.9	313.6	0.87	10.34	10.55	2.03
9	310.9	307.4	-1.15	6.89	6.67	-3.19
10	306.3	306.2	-0.03	4.90	4.92	0.41
11	307.3	307.1	-0.06	4.93	4.95	0.41
12	307.6	307.8	0.06	4.96	4.97	0.20
13	308.6	308.5	-0.03	4.96	4.99	0.60
14	397.2	399.9	0.71	5.60	5.77	3.04
15	428.8	428.0	-0.19	4.19	4.25	1.43
16	436.3	435.3	-0.23	3.85	3.98	3.37
17	442.6	440.1	-0.56	3.90	3.94	1.03
18	449.4	449.4	0.00	3.81	3.85	1.05
19	450.2	450.8	0.14	3.88	3.88	0.00
20	405.9	408.1	0.54	5.11	5.36	4.89
21	417.9	420.3	0.58	4.51	4.66	3.33
22	387.0	391.2	1.07	7.22	7.65	5.96
23	385.4	388.0	0.67	5.62	6.04	7.47

Figure Captions:

Fig.1(a) Critical lines for binary mixtures of methane and propane(C_1-C_3). Triangles: experimental critical temperatures; Circles: experimental critical pressures; Solid lines: EOSCF+RG. Dashed lines: EOSCF.

Fig.1(b) *P-T* loci for binary mixtures of methane and propane (C_1-C_3). Left line is for pure C_1; right line is for pure C_3; the line connecting C_1 and C_3 is the critical locus for the mixture. Squares: experimental data; dark circles: critical points of pure C_1 and C_3 calculated from EOSCF+RG; dark diamonds: critical points of pure C_1 and C_3 calculated from EOSCF; Solid lines: EOSCF+RG. Dashed lines: EOSCF.

Fig.2(a) Critical lines for binary mixture of ethane and *n*-butane (C_2-C_4). Legend as in Fig.1(a).

Fig.2(b) *P-T* loci for binary mixtures of ethane and *n*-butane (C_2-C_4). Legend as in Fig.1(b).

Fig.3(a) Critical lines for binary mixtures of *n*-butane and *n*-hexane (C_4-C_6). Legend as in Fig.1(a).

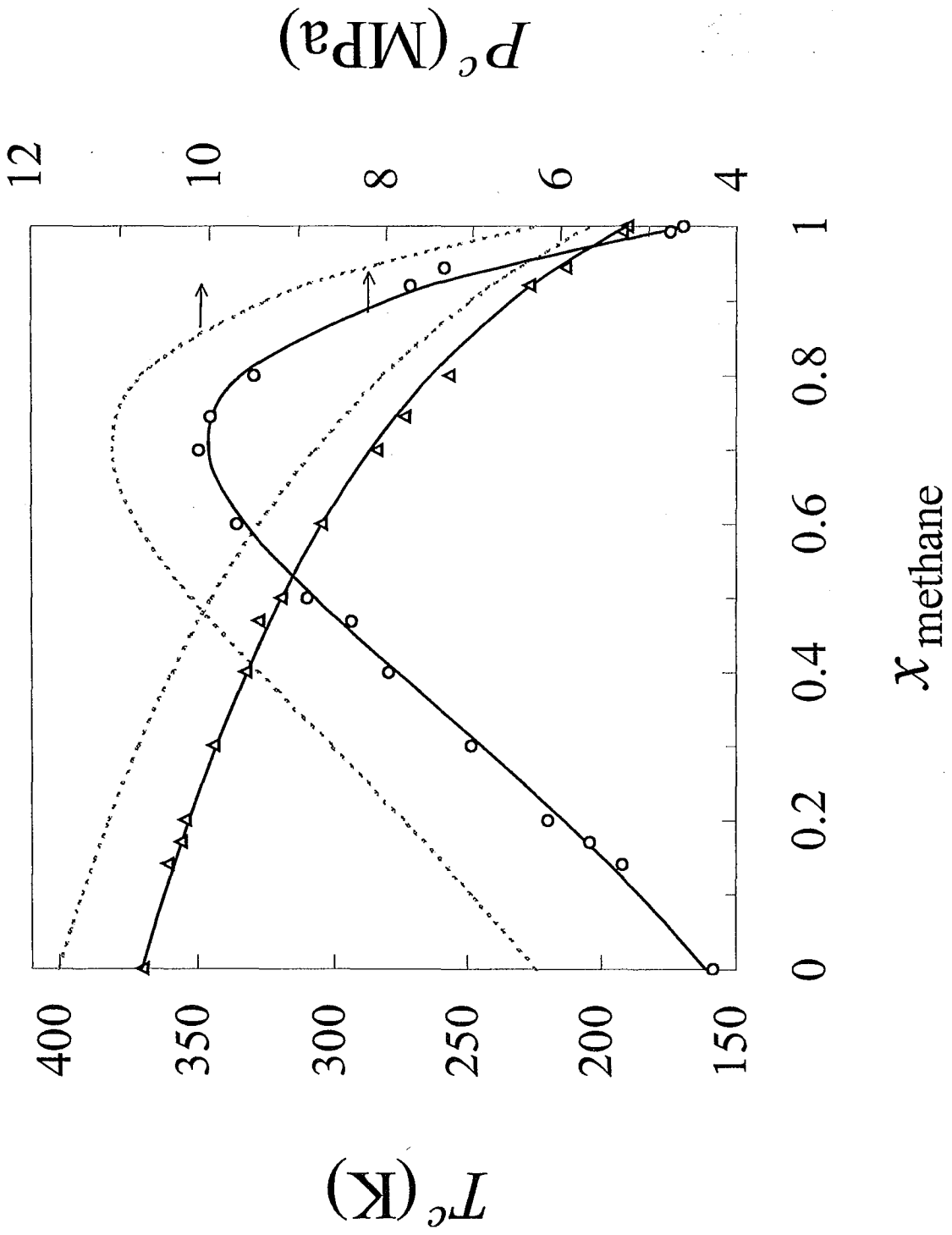Fig.3(b) *P-T* loci for binary mixtures of *n*-butane and *n*-hexane (C_4-C_6). Legend as in Fig.1(b).
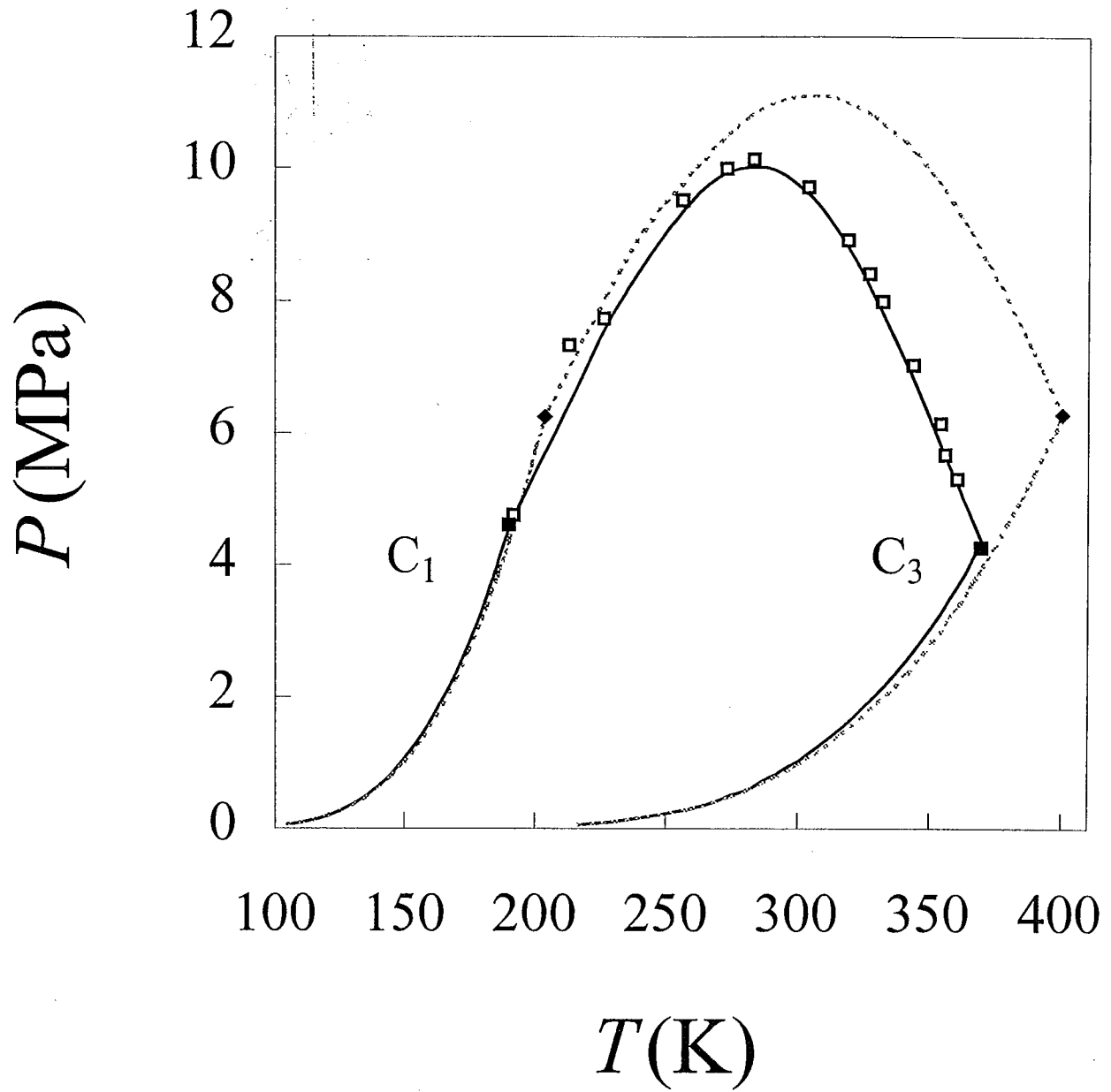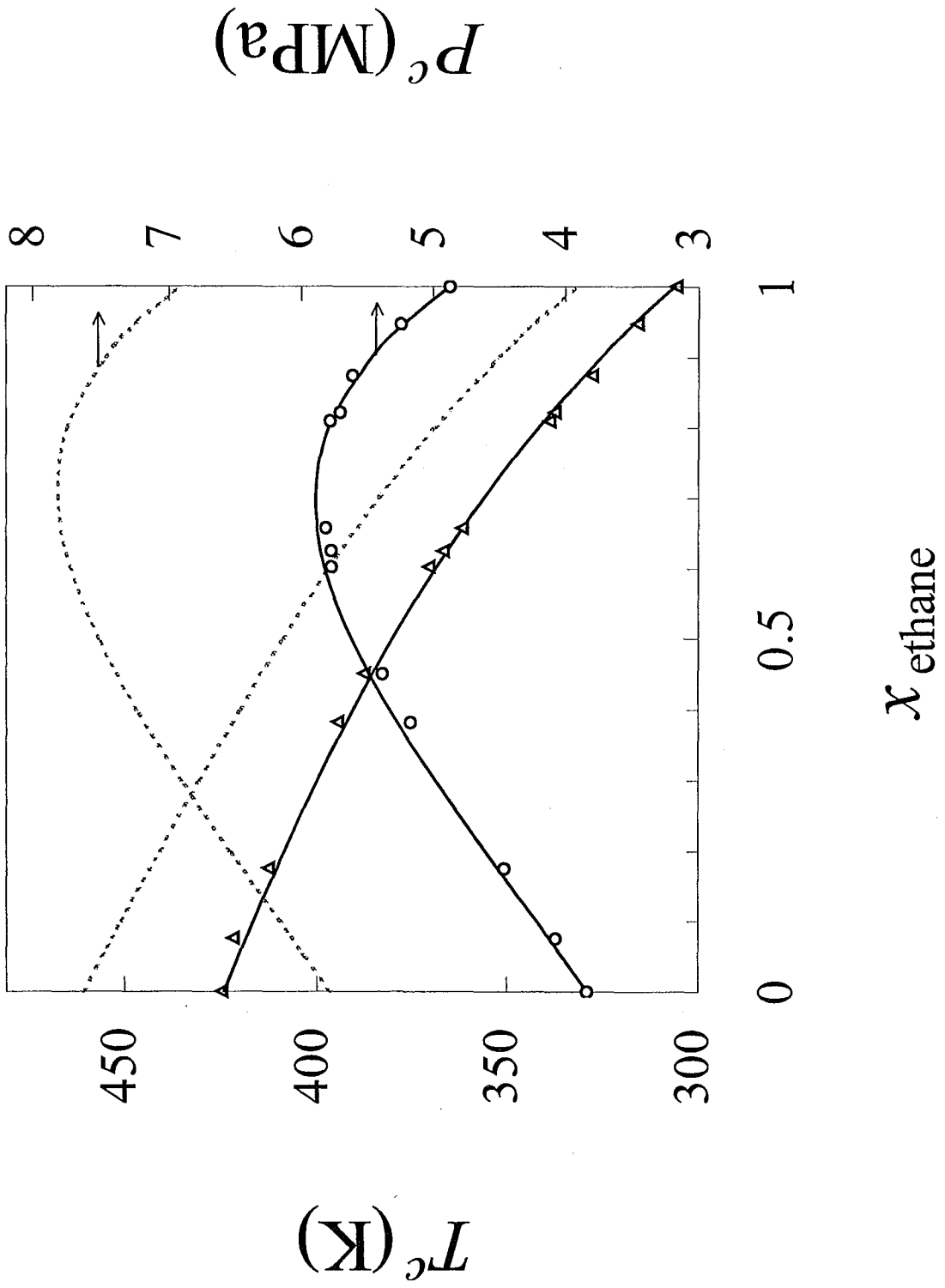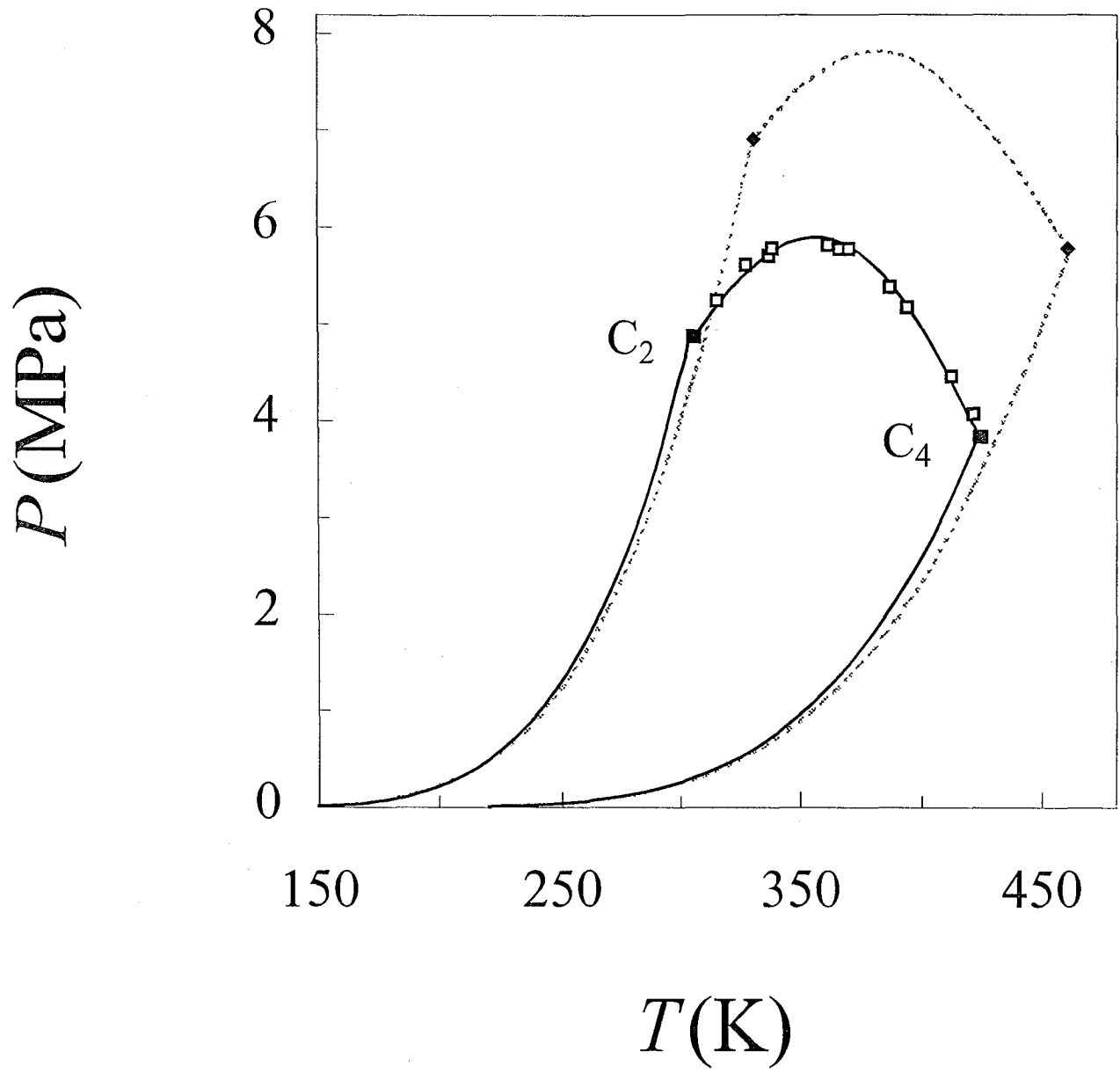
Fig. 1(a)

Fig.1(b)

Fig. 2 (a)

Fig. 2(b)

Fig. 3 (a)

P^c (MPa)

T^c (K)

x_n -butane

Fig. 3(b)

C_4

C_6

P (MPa)

T (K)